Inelastic electron scattering by a molecule embedded in a host medium: Role of the electronic structure of the medium

D. C. Marinica, D. Teillet-Billy, and J. P. Gauyacq
Laboratoire des Collisions Atomiques et Moléculaires, UMR CNRS-Université Paris-Sud 8625, Bât. 351, Université Paris-Sud, 91405 Orsay Cedex, France
(Received 15 October 2004; published 31 March 2005)

The electron impact excitation of a molecule located inside a dielectric medium is theoretically studied. Electronic excitation of an O_2 molecule embedded in pieces of a Ne fcc crystal of variable size is calculated. The Ne medium is described using a microscopic model. The structures that appear in the energy dependence of the inelastic scattering probabilities are related to the electronic properties of the host medium. They are assigned either to the bulk medium electronic properties or to quantization effects in the finite size cluster. In the present case, the electron impact excitation probability is shown to directly reflect the host medium density of electronic states.

DOI: 10.1103/PhysRevB.71.115438 PACS number(s): 79.20.Uv, 34.80.Gs, 77.22.−d, 73.22.−f

I. INTRODUCTION

A molecule can be excited by collisions of low energy electrons. Vibrational as well as electronic excitation can be very efficiently induced in particular when transient negative ion intermediates are formed in the course of the electron collision.[1] The formation of short lived negative ion resonances has been found to be the dominant mechanism for efficient energy transfer from a low energy electron to a molecule, for isolated molecules[1] as well as for molecules located near solid environments.[2–4] However, in the latter case, one can wonder about the role of the surrounding medium in electron-molecule energy transfer and more generally of its importance for the electron-induced reactivity: does the environment of a molecule favor or unfavor the electron-induced reactivity? In this context, a probe molecule physisorbed on top of a solid surface or inside a host medium is a very attractive system to study for the understanding of the role of the environment; a physisorbed molecule is hardly perturbed by the environment and the surrounding medium only affects the electron scattering properties, so that the study concentrates on the host medium effect. The case of a molecule physisorbed on a solid metal surface has been the subject of several detailed studies (see, e.g., references in Refs. 2–4). In this case, significant modifications of the inelastic scattering processes[5,6] have been observed and rationalized in terms of a reduction[7–10] or an increase[11–13] of the lifetime of the negative ion intermediates as compared to the isolated molecule case; the important role of the asymmetry introduced by the metal-vacuum interface has also been stressed.[9,10]

Recently, experimental studies of electron impact excitation of molecules located inside a thick dielectric layer condensed on a metal substrate have been reported.[14,15] The rich structures that appear in the dependence of the inelastic processes on the electron incident energy have been related to the electronic properties of the host medium. Similarly, earlier studies of the electron impact phonon excitation in condensed Ar have also shown strong correlation with the bulk Ar density of electronic states.[16,17] The interpretation of these experimental studies have involved different effects:[18] probability for the electron to enter and leave the dielectric medium, transport through the medium, effects of the medium density of states. Depending on the process under discussion, these effects lead to a direct or inverse correlation between the excitation probability and the host medium density of electronic states.

The purpose of the present theoretical study is to illustrate the role of the electronic structure of the host medium in an inelastic electron scattering process. A simple and realistic probe system is built for this purpose; it consists in an oxygen molecule embedded inside a dielectric host medium, a piece of Ne crystal. Ne has been chosen as the host medium for computational convenience. We show that the electronic excitation of the O_2 molecule by electron impact inside a finite size Ne crystal directly reflects the density of electronic states of the Ne solid and the quantization effects due to the finite size of the embedding medium.

The paper is organized in the following way. Section II presents the model system and Sec. III its theoretical description. Section IV presents the results for the excitation probability by electron impact of the oxygen molecule embedded in a finite size Ne solid together with a discussion of these results in terms of density of electronic states of the host medium. This leads to conclusions developed in Sec. V.

II. MODEL SYSTEM: ELECTRONIC EXCITATION BY ELECTRON IMPACT OF AN OXYGEN MOLECULE EMBEDDED IN A RARE GAS CLUSTER

The present work studies inelastic scattering of low energy electrons by a probe system, formed by a molecule inside a host medium. The target is an oxygen molecule embedded inside a Ne crystal of variable finite size. The excitation from the ground electronic state $O_2(\pi_g^2)X\,^3\Sigma_g^-$ to the two first excited states $O_2(\pi_g^2)a\,^1\Delta_g, b\,^1\Sigma_g^+$ is very efficiently induced by electron impact at low energy. For a free O_2 target, this process extends from threshold to tens of eV

and presents, to a large extent, a structureless energy dependence. It has been carefully studied both experimentally[19–21] and theoretically.[22–24] The case of O_2 molecules physisorbed on metal surfaces has also been studied.[25,26] The $(X \rightarrow a)$ and $(X \rightarrow b)$ electronic excitations correspond to spin forbidden transitions and require an electron spin exchange between the target and the collisional electron. This is very efficiently performed via a two-step resonant mechanism, in which the incident electron couples to the target molecule to form a $O_2^-(\pi_g^3)$ resonance of $^2\Pi_g$ symmetry and the outgoing electron is any of the three equivalent π_g electrons of the resonant intermediate, leading to the formation of the three states of the $O_2(\pi_g^2)$ configuration. This two-step excitation mechanism is resonant but with a meaning that differs from the usual one,[22] since it is not mainly active at the resonant energy (the inelastic channels are closed at this energy) but in an extended energy range in the high energy wing of the resonance.

The host material is chosen as a piece of an fcc Ne crystal, with the bulk lattice parameter. To characterize the role of the electronic structure of the host medium in the excitation process, a series of calculations were performed considering larger and larger pieces of Ne crystal. Calculations with Ne can be performed on larger sized clusters than for other rare gas (see discussion at the end of Sec. III B), motivating the present choice of Ne as the host medium. The Ne host was defined as all the Ne atoms of an fcc crystal located inside a sphere of given radius. The probe molecule is at the center of this quasispherical cluster; it is located either at an insertion or at a substitution site of the crystal and is surrounded by an increasing number of shells of rare gas atoms (a shell is defined as the ensemble of Ne atoms at the same distance from the center of the cluster). The systems correspond for the smallest size to the shell formed by the first nearest neighbors around the probe molecule and for the largest size to a cluster of around 600 atoms. With this stepwise construction, the electronic structure of the medium changes with the size of the Ne cluster (in particular, as shown below, finite size quantization effects occur) and the corresponding changes in the energy dependence of the oxygen excitation probability by electron impact are studied. It must be stressed that our purpose was to build step by step a piece of bulk material of fcc structure and not to study the case of a molecule embedded inside a real rare gas cluster. As discussed in Ref. 27, small clusters generally exhibit an icosaedral structure. Nevertheless, for convenience, below we call clusters the pieces of fcc Ne crystal we consider.

III. THEORETICAL APPROACH

Electronic excitation by electron impact is calculated and the influence of the electronic structure of the host medium is studied directly on the excitation probability. The electron is scattered by the compound system formed by the molecule and the rare gas atoms that form the cluster or molecular solid. The potential that scatters the electron is the superposition of the interaction potential of the electron with the molecule and with all the individual rare gas atoms. The electron is elastically scattered by the rare gas atoms but inelastically scattered by the molecule located inside the piece of Ne solid. The description is based on the coupled angular mode (CAM) method.[28,9] This method is able to describe elastic and inelastic electron scattering by a nonspherically symmetric potential. In particular it can describe inelastic electron molecule scattering by a multichannel effective range theory approximation. Such a method has been already used in previous works in particular to treat electronic excitation by electron impact of O_2 molecule physisorbed on a metal surface.[25]

A. Electron-Ne interaction

A model potential has been determined to describe the electron interaction with a single free Ne atom. This potential has been built to reproduce the properties of electron scattering by a Ne atom at low energy. A local expression of the potential only function of the electron-atom distance r and independent of the electron angular momentum ℓ has been used,

$$V(r) = A_0 \exp(-A_1 r^2) - \frac{\alpha}{(r^2 + A_2)^2}. \quad (1)$$

It includes a long range polarization interaction (polarizability $\alpha = 2.66 a_0^3$), with a saturation term $A_2 = 1.0 a_0^2$. The (A_0, A_1, A_2) parameters have been adjusted to reproduce the s, p, and d phase-shifts ($A_0 = 2.5$ and $A_1 = 0.7$ in atomic units) in the few eV energy range. The agreement between the phase-shifts calculated with the adjusted present model potential and phase-shifts as given in the literature in the 0 to 6 eV range[29–32] is quite satisfactory. A similar approach has been adopted earlier for the electron-Ar potential.[33,34] The present electron-Ne model potential is not as attractive as the e-Ar potential in Refs. 33,34. In particular, it does not bind any core level.

The quality of the electron-Ne model potential is checked by computing the band structure of the bulk medium and in particular by determining the energy position of the bottom of the Ne conduction band. Two calculations have been performed either including or not including the mutual polarization of atoms (see the discussion in Ref. 34). Each rare gas atom is polarized by the collisional electron and also by all the other rare gas atoms. This last term occurs through the electron induced dipoles on all the other rare gas atoms. The electric field on each rare gas atom is then obtained via a self-consistent procedure (see Ref. 34). This mutual polarization of the Ne atoms corresponds to the Ne atoms screening the field of the collisional electron, i.e., to the dielectric character of the Ne solid. The calculated band structure, with the mutual polarization fully included, is in good agreement with previous calculations.[35] The bottom of the conduction band is found at 1.06 eV above vacuum in agreement with recent (1 eV in Ref. 36) and older (1.4 eV in Refs. 37,38) measurements. The effective mass of the electron at the bottom of the conduction band has also been computed; it is found to be approximately equal to the free electron mass $(m^* = 1.03 m_e)$. The influence of the mutual polarization of Ne atoms is estimated by running a similar calculation but

without including the mutual polarization. This increases the attractive strength of the polarization potential and leads to a decrease by 0.11 eV of the energy of the bottom of the conduction band with respect to the vacuum level; the effective mass is unchanged. Minor changes in the shape of the band structure also appear. In the present study on Ne clusters, the mutual polarization is not included in the calculation and only minor effects on the excitation probability are expected from this approximation.

B. CAM (coupled angular mode) approach

The CAM method is a scattering method developed for the description of scattering of electrons by a nonspherically symmetric potential $V(\vec{r})$,

$$[T + V(\vec{r}) - E]\psi(\vec{r}) = 0. \tag{2}$$

In the present case, $V(\vec{r})$ is the superposition of the electron molecule potential and of the individual electron atom model potentials. The Schrödinger equation (2) is solved in spherical coordinates centered at the molecule. The electron wave function is expanded over an angular basis formed by spherical harmonics centered at the molecule $Y_{\ell m}(\hat{r})$ and characterized by the electron momentum ℓ and its projection, m, on the quantization axis, taken along the molecular axis. The total wave function for the collisional system is then written as the following expansion over the $(\lambda, \ell m)$ channels associated with the electronic states ϕ_λ of O_2 defined below

$$|\Psi\rangle = \sum_\lambda \sum_{\ell m} \frac{1}{r} Y_{\ell m}(\hat{r}) \mathrm{F}^\lambda_{\ell m}(r) |\phi_\lambda\rangle, \tag{3}$$

where the $F^\lambda_{\ell m}(r)$ are the corresponding radial wave functions for the collisional electron. The nonspherical interaction $V(\vec{r})$ felt by the electron around the molecular center due in particular to the presence of the rare gas atoms induces couplings between the spherical harmonics. Due to these couplings, the radial parts $F^\lambda_{\ell m}(r)$ of the electron wave function are given by a system of coupled equations that is solved by propagation. This requires to propagate the radial part of the electron wave functions from the molecular center to the region outside the Ne cluster, that is to say beyond all of the electron atom potentials. An extended angular basis must then be used to properly describe the wave function.

The electron molecule interaction is treated in the multichannel effective range theory (ERT) approximation.[39] This description for the electronic excitation has been described in detail in previous works.[22,25] In the ERT approach, the electron space is cut in two regions, an inner region inside a sphere centered on the molecule and an outer region. Expansion (3) is used in the outer region and matches the wave function of the inner region. The inner region is not explicitly described in this approach and is replaced by a boundary condition for the wave function in the outer region. For the oxygen molecule, the ERT boundary conditions are given in Ref. 22. The coupled equations for the radial electron wave functions are solved in the outer region from the inner region boundary up to large radial distance where the scattering S matrix is extracted. The excitation "probability" $P_{\lambda\to\lambda'}$ from the λ to the λ' electronic states is given by

$$P_{\lambda\to\lambda'} = \sum_{i,j} |S_{ij}^{\lambda\to\lambda'}|^2, \tag{4}$$

where i and j are angular mode indexes. $P_{\lambda\to\lambda'}$ expresses the strength of the excitation process and enters the expression of the excitation cross section together with a flux term (proportional to the inverse energy) and statistical factors. The excitation probabilities are computed for the present model system and discussed.

Our purpose here is to demonstrate that an inelastic process induced by electron impact reflects the electronic properties of the host medium. In that perspective, a "reduced" version of the O_2 electronic excitation description has been adopted.[22] This version only includes (as ϕ_λ channels) the three electronic states ($X\,^3\Sigma_g^-$, $a\,^1\Delta_g$, and $b\,^1\Sigma_g^+$) corresponding to the π_g^2 configuration. It does not include the six electronic states associated with the $(\pi_u^3\pi_g^3)$ configuration and corresponding to the decay of the $(\pi_u^4\pi_g^3)^2\Pi_g$ resonance by ejection of a π_u electron. The main advantage of this "light" version is to significantly reduce the size of the propagation matrix (the number of coupled electronic channels is reduced from 9 to 3) then allowing to increase the size of the Ne clusters which can be considered. In this reduced version, the excitation probabilities to the π_g^2 channels are larger than in the full calculation.[22] This is not surprising since in the "light" version the resonance cannot decay into the $\pi_u^3\pi_g^3$ channels and the outgoing flux is then only shared among the three π_g^2 final channels.

Site effects have been considered with the molecule located either in an insertion site at the center of the fcc cubic cell or in a substitution site with the molecule replacing one of the Ne atoms of the fcc lattice. In both cases, the molecular axis is oriented along the $<100>$ direction, which is chosen as the z-axis for the spherical harmonics definition. This orientation preserves the high symmetry of the compound (molecule+cluster) system. This choice of orientation limits the computational demand without resulting in a model system with too specific a behavior as discussed below. With these choices of location and orientation of the molecule, the symmetry of the surrounding medium is such that the electron-medium interaction potential can only induce couplings between spherical harmonics with angular momentum such that $\Delta\ell$ and Δm are even numbers. For any other orientation, these selection rules would be lifted. Furthermore, since the resonant excitation implies the capture of a $d\pi$ electron, only even angular momenta ℓ and odd values of its projection m on the molecular axis can contribute to the excitation process.

With the present (O_2 in Ne) system, convergence of the calculation of the scattering wave functions (three electronic states and spherical harmonic expansion up to $\ell = 30$) can be reached for the case of clusters as large as 600 atoms occupying a sphere of 25 Bohr radius. One can stress that the

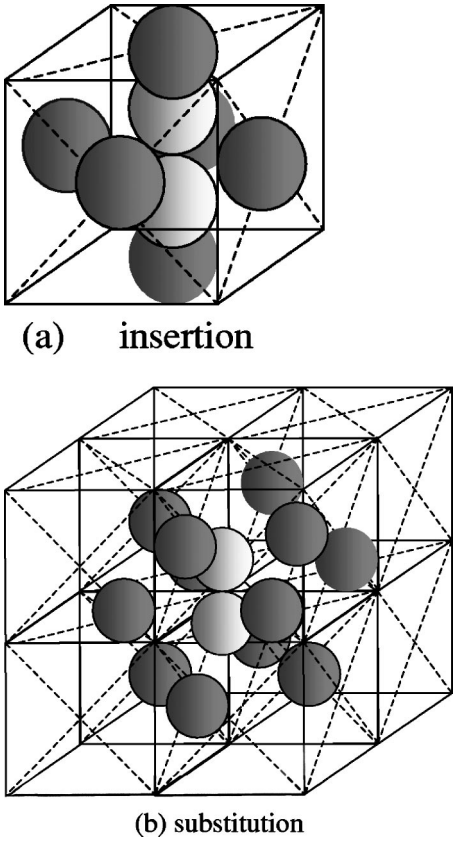

FIG. 1. Schematic representation of a diatomic molecule (light gray spheres) at the center of one-shell rare gas fcc clusters (only the first nearest neighbors of the molecule: dark gray spheres) at an insertion site (a) or at a substitution site (b).

choice of Ne as the host medium has several advantages that make convergence possible for clusters of significant size. The main point concerns the model potential (1) describing the *e*-Ne interaction which does not bind core levels. This means that the magnitude of the potential is moderate and that the description of the electron scattering wave function does not need very small spatial steps (radial and angular), as it would in the case of potential binding core levels. The choice of Ne as the host medium then makes possible a converged calculation for rather large clusters, large enough to allow a discussion of the excitation probabilities in terms of Ne bulk electronic structure.

C. Excitation probability and density of electronic states

O_2 excitation has been calculated for electron impact energy from threshold up to 12 eV. This calculation is quite similar to the calculation performed for O_2 molecule physisorbed on a metal substrate (see further details in Ref. 25). The O_2 molecule is located at both insertion and substitution sites inside clusters of one to 17 shells of Ne. Figures 1(a) and 1(b) schematically present the location of the nearest rare gas neighbors (first shell of Ne atoms around the molecule) for a molecule embedded, respectively, at an insertion [Fig. 1(a)] or a substitution [Fig. 1(b)] site.

In order to interpret the results for the excitation probability, calculations of elastic scattering of an electron by Ne clusters without the O_2 molecule, have also been performed using the same CAM approach. The electron wave is then only scattered by the atoms of the medium. For a spherically symmetric target, scattering can be described by one phase-shift for each spherical wave. The associated time delay $\tau=\hbar(d\delta_\ell/dE)$ is related to the energy dependence of the phase-shifts δ_ℓ. It brings information on the energy position of resonances and allows the extraction of their width. The time delay can also be related to the change in the density of states induced by scattering (see for instance in Ref. 40). In the present case, the scattering is not spherically symmetric and scattering is represented by a scattering matrix *S*. The energy dependence of this matrix leads to the generalized time delay matrix[41] $Q=(\hbar/2i)S^+(dS/dE)$. The *S* and *Q* matrix generalize the above properties of the phase shifts. Using the CAM approach for the cluster without the O_2 molecule, one can get the scattering *S* matrix and the time delay matrix, *Q*. The difference between the traces of the time delay matrices calculated with and without the cluster of atoms then reflects the changes induced by the cluster. In particular, peaks in the trace difference as a function of collisional energy point at the location of the quasistationary states of the system.[10,28] This calculation is performed using the same angular momentum expansion, i.e., the same symmetry restriction as that used in the study of the O_2 electronic excitation probability. This then allows a direct discussion of the effect of the cluster electronic structure on the electron impact excitation.

Finally, the total density of states of bulk Ne has also been computed for the present approach neglecting the mutual polarization of the Ne atoms. This is performed by diagonalization of the electron-Ne interaction potential in a plane wave basis. The corresponding total density of states is also used below in the discussion of the electronic excitation of the embedded molecule. This bulk total density of states does not include the symmetry restriction imposed by the resonance, in contrast with the above discussed calculations of the time delay for a finite size cluster.

IV. RESULTS AND DISCUSSION

A. Excitation probability by electron impact of an oxygen molecule embedded in a rare gas cluster

Figures 2(a) and 2(b) present the probability for the electron impact excitation of the isolated molecule from the ground state to the two first excited states (*X*-*a* and *X*-*b*) from their energy threshold (0.98 eV for the *X*-*a* transition, 1.65 eV for the *X*-*b* transition) up to 12 eV. In the case of an isolated molecule, the excitation probabilities are rather large, they reach 0.4 and 0.2, respectively, at 12 eV. The factor 2 between them corresponds to the factor 2 between the corresponding parentage coefficients.[22,42,43] These are equal to 3/2, 1, and 1/2 for the X,a, and *b* states, respectively. In the present model description of the O_2 electronic system, the opening of the π_u shell has not been included and this leads to an overestimation of the excitation probabilities to the *a* and *b* states by roughly a factor $(7/3)^2$ corresponding to the squared ratio between the number of involved electrons.[22,43]

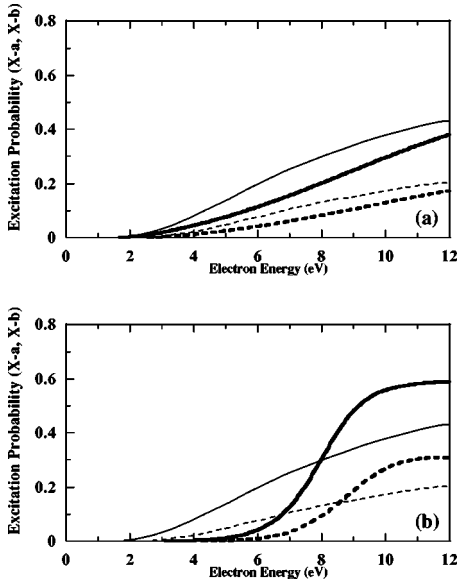

FIG. 2. (a) Excitation probability from the ground state $O_2(\pi_g^2)X\,^3\Sigma_g^-$ to the first two excited states of $O_2(\pi_g^2)a\,^1\Delta_g$ and $b\,^1\Sigma_g^+$ as a function of the electron impact energy (eV). Comparison of the excitation probabilities for a free molecule to a molecule at an insertion site surrounded by a one-shell Ne cluster (only the nearest Ne neighbors). Full line, *X-a* excitation; dotted line, *X-b* excitation; thick lines for the embedded molecule; thin lines for the free molecule. (b) Same as (a) for the substitution site.

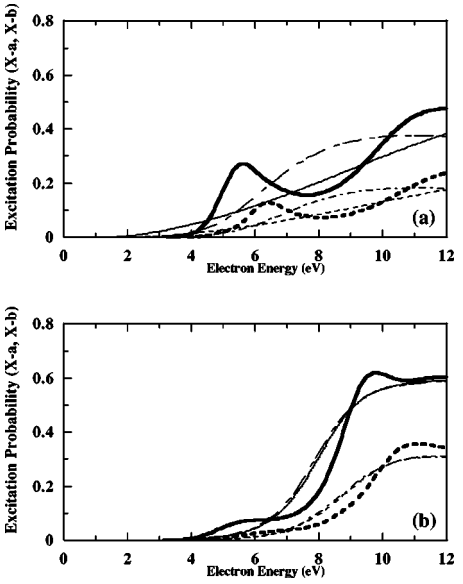

FIG. 3. (a) Excitation probability from the O_2 ground state to the $a\,^1\Delta_g$ and $b\,^1\Sigma_g^+$ excited states as a function of the electron impact energy (eV). Comparison of the excitation probabilities for a molecule at an insertion site surrounded by a one-, two- or three-shell Ne cluster. *X-a* excitation, one-shell cluster (thin full line), two-shell cluster (dashed-dotted line), three-shell cluster (thick full line). *X-b* excitation, one-shell cluster (thin dotted line), two-shell cluster (short dashed-dotted line), three-shell cluster (thick dotted line). (b) Same as (a) for the substitution site.

Figures 2(a) and 2(b) also present the excitation probability for a molecule surrounded by the first Ne shell formed by the nearest Ne neighbors (see a schematic picture in Fig. 1). The molecule is located either in an insertion site [Fig. 2(a)] at the center of the conventional cubic cell of a fcc crystal, or in a substitution site [Fig. 2(b)]. The number of neighbors is then, respectively, six or 12 Ne atoms [see in Figs. 1(a) and 1(b)]. The radius of this first "shell" is either $4.2a_0$ (insertion site) or $6.0a_0$ (substitution site), with a cell parameter, the fcc cube side, equal to $8.4a_0$. For the insertion site, the Ne atoms are located on the x,y, and z axis of the CAM reference frame and thus in the nodal planes of the resonant π_g orbital. For the substitution site, only four Ne atoms (out of 12) are located in the resonant π_g orbital nodal plane.

The general features found for both adsorption sites are the following: the magnitude of the excitation probability does not change much compared to the isolated molecule case, it is however smaller in the threshold energy range. In the insertion case, the first shell of nearest Ne neighbors does not induce strong modifications in the excitation probability. This is not much surprising since all the Ne atoms are localized in the nodal planes of the O_2^- resonance and the short range and the long range parts of the electron-Ne interaction are not very strong. The situation is somewhat different in the substitution case and the shape of the excitation probability is changed compared to the isolated molecule case. In that case, eight Ne atoms (among the 12) are in the lobes of the resonant π_g orbital and then influence the excitation probability more efficiently than in the insertion site case.

Figures 3(a) and 3(b) compare the inelastic excitation probabilities for the O_2 molecule embedded in Ne clusters formed of one, two or three shells of nearest atoms, with the molecule either at an insertion [Fig. 3(a)] or substitution [Fig. 3(b)] site. The three-shell clusters built around an insertion or substitution sites contain 42 and 38 Ne atoms, respectively. The magnitude of the excitation probabilities is not modified by this increase of the cluster size. However, for both sites, the three-shell cluster results exhibit marked structures in the energy dependence of the excitation probabilities with maxima around 6 and 9–11 eV. These structures appear with the third shell in both cases, although slightly shifted. It can be stressed that for the substitution site the second shell does not induce any modification compared with the one shell cluster and that important modifications in the shape of the excitation probabilities only appear with the third shell.

Figures 4(a)–4(d) present the inelastic excitation probabilities for larger clusters of nine and 17 shells of Ne atoms around the insertion and substitution sites. These clusters contain, respectively, 236 and 610 Ne atoms (insertion case) and 176 and 458 Ne atoms (substitution case). A shifted energy threshold for the excitation probability is observed for both molecular sites, an effect that was already present in smaller clusters. For a molecule at the insertion site, the excitation probability to the a state presents well-marked structures with two broad maxima around 6 and 10 eV. Inside these broad peaks, the excitation probabilities also exhibit many peaks with a small amplitude. Their number increases when increasing the cluster size from nine to 17 shells. Be-

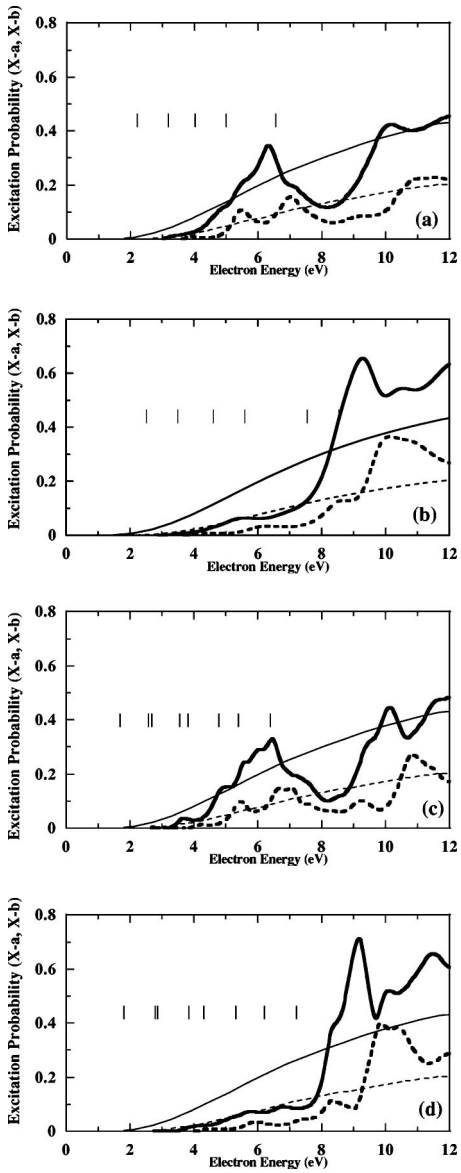

FIG. 4. Excitation probability from the ground state to the two first excited states $a\ ^1\Delta_g$ and $b\ ^1\Sigma_g^+$ of O_2 as function of the electron impact energy. Full lines for the *X-a* excitation, dotted lines for the *X-b* excitation, thick lines for the embedded molecule, and thin lines for the free molecule case. Vertical short ticks point to the successive quantized energies in the $\ell=2$ symmetry for the incident and inelastic *X-a* channel. (a), (c) The O_2 molecule is located in an insertion site of the rare gas fcc crystal; the molecule is surrounded by the rare gas atoms corresponding to the first nine (a) and first 17 (c) shells of nearest neighbors. (b), (d) The O_2 molecule is located in a substitution site of the rare gas fcc crystal; the molecule is surrounded by the rare gas atoms corresponding to the first nine (b) and first 17 (d) shells of nearest neighbors.

low, we will show that these structures can be related to the electronic structure of the Ne cluster. In particular the small amplitude oscillations in the probabilities are attributed to the quantization of the electron motion in the finite size cluster. The larger the cluster radius, the smaller the energy period of these oscillations. The vertical bars point to quantized energy values calculated with a model described below. Similar structures are observed for clusters with a molecule at the substitution site [Figs. 4(b) and 4(d)]. However, in this case, the overall energy shape of the excitation probabilities is quite different. The excitation probabilities keep rather small below 8 eV and increase abruptly between 8 and 9 eV for the excitation to the a state, reaching a value as high as 0.7. One can stress that due to the competition between exit channels, a large excitation probability in one channel cannot be associated with a large probability in the other. This competition effect is probably playing a role in the delayed increase of the *b*-excitation at 10 eV, as compared to the *a*-excitation.

Comparison between clusters of different size (1,3,9,17 shells) shows that the overall energy dependence of the excitation probabilities builds up starting from the three shells case; beyond, the increase of the cluster size only leads to minor modifications, except for the oscillations due to the finite size of the cluster. This overall energy shape results from the specificity of the O_2 molecule excitation, the coupling of the O_2^- resonance with its environment and the bulk properties of the rare gas solid. Below we discuss in more detail the relation with the electronic structure of the Ne cluster.

B. Discussion

The present excitation probabilities are not so easy to interpret since several effects are involved. In such an excitation process, the incident electron has first to enter the cluster, to propagate through the cluster, i.e., to be scattered elastically by the Ne atoms, to suffer an inelastic scattering by the molecule and to again propagate through the cluster and be scattered back into vacuum at an energy different from the incident one. This means that the electronic properties of the medium appear twice in the excitation probability: once at the incident energy and once at the final energy. Furthermore, in a two excited channel system, competition between the two channels is also present. To better interpret these different effects, we examine below the density of electronic states of the Ne cluster as a function of the energy.

First, let us consider the total density of states of bulk Ne shown in Fig. 5. It has been computed for an infinite Ne crystal, using the potential (1) but without the mutual polarization of the Ne atoms taken into account, i.e., with the same Ne description as the above inelastic scattering calculations. However, it is the total density of states, without the symmetry restriction appearing in the molecular excitation process discussed above. This density of states has been computed with a finite number of *k* values and it has been convoluted with a Gaussian function of FWHM equal to 80 meV to remove possible artefacts brought by this finite calculation. In Fig. 5, one recognizes the conduction band of Ne starting at 0.98 eV above vacuum and exhibiting the parabolic structure of a quasifree electron band at low energy (the black dots line is a parabola starting at the bottom of the conduction band and adjusted to the low energy part of the present density of states). Above, it exhibits two well-marked broad peaks at 6 eV and 9.5 eV, separated by a broad mini-

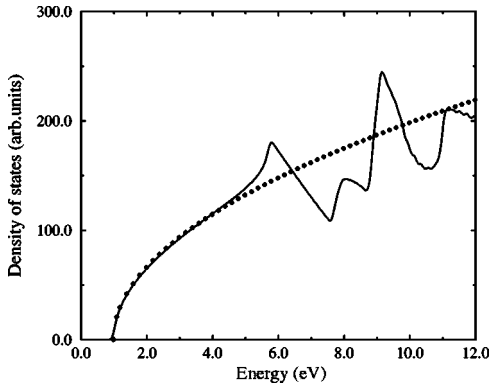

FIG. 5. Total density of states of bulk Ne as a function of the electron energy above vacuum level. Full line, total density of states (arbitrary units). Dotted line, parabola adjusted to the low energy density of states.

mum. This broad minimum in the density of states is located in the energy range of the *X*- and *L*-band gaps and also appears in LDA calculations.[35] It is thus a characteristic of the Ne bulk density of states.

Figures 6(a)–6(d) present the difference between the traces of the time delay matrices calculated with and without the cluster of atoms. The calculation is performed in the CAM approach, using the same symmetry restrictions as for resonant scattering. The scattering center is located either at an insertion site or at a substitution site and the cluster size is nine or 17 shells. These calculations then correspond to the same symmetry as the inelastic probabilities in Fig. 4. Two main features appear in all the results in Figs. 6(a)–6(d) (nine or 17 shells, insertion or substitution site), a minimum in the 7–8 eV range, corresponding to the minimum observed in Fig. 5 in the total density of states and a series of peaks in the energy range where the total density of states is parabolic, i.e., free-electron like. We interpret the peaks in the low energy region as quasistationary states that are a consequence of the finite size of the Ne cluster, i.e., a consequence of quantization inside the cluster. The electron wave inside the cluster is partially reflected at the cluster border. Quantized levels appear when the reflected electron waves interfere constructively. The period of the oscillations in Fig. 6 varies with the cluster size: the larger the size of the cluster, the shorter the oscillation period. The cluster radius is $19.3a_0$ for the nine-shell and $27.6a_0$ for the 17-shell cluster around an insertion site and $17.9a_0$ and $25.3a_0$ for the corresponding clusters around a substitution site. The oscillation period approximately changes as the square of the inverse of the cluster radius.

To further confirm the origin of these oscillations and to assign the corresponding peaks, we estimated the peak position by a simple model. The rare gas cluster is considered as a sphere of radius R in which the electron is moving freely. As the simplest view as possible, it is assumed that the sphere radius R is equal to the radius of the shell of the outermost rare gas atoms, the potential inside the cluster is constant and equal to $V_0(R)$ and the electron mass is equal to the free-electron mass, m_e. Quantized states for the electron inside such a sphere are then associated with

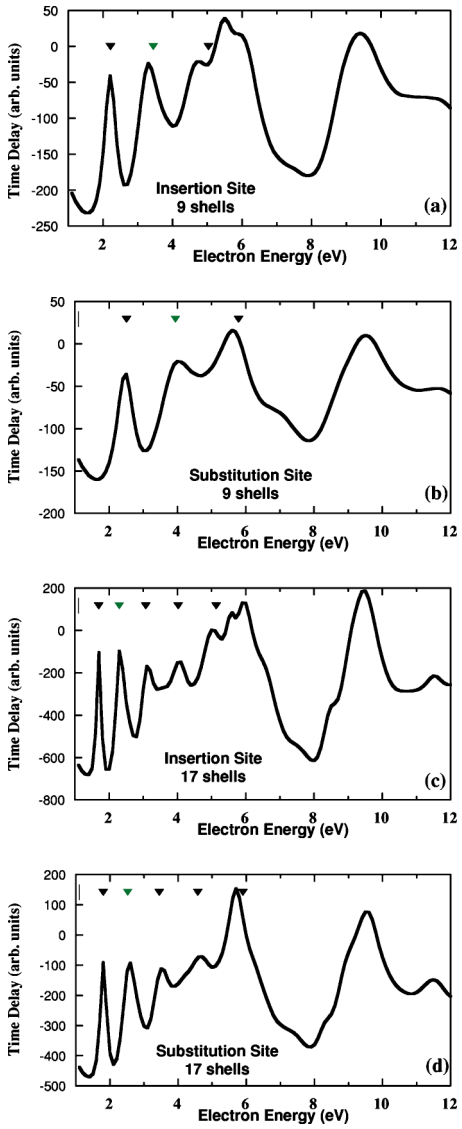

FIG. 6. Time delay calculation (difference of the trace of the time delay matrix obtained in CAM calculations with and without the Ne cluster). (a), (c) Calculated at an insertion site of the rare gas fcc crystal with nine (a) or 17 (c) shells of rare gas atoms. (b), (d) Calculated at a substitution site of the rare gas fcc crystal with nine (b) or 17 (d) shells of atoms. The symbols point to the properties of the sphere model. Vertical bars, constant potential energy $V_0(R)$, bottom of the effective conduction band in the cluster. Full triangles, energies of the first quantized levels in the $\ell=2,4,6,8$ symmetries.

the successive zeros of the $\ell=2$, 4, … spherical Bessel functions at the sphere radius (the ℓ restriction comes from the symmetry restriction of this calculation). Their energies are

$$E(\ell,R) = V_0(R) + \frac{1}{2m_e}\left(\frac{z_\ell}{R}\right)^2, \tag{5}$$

where z_ℓ is the first zero of the spherical Bessel function of index ℓ.

Symbols have been drawn in Fig. 6, that point to the quantization energies obtained by the above model. The constant potential inside the sphere, $V_0(R)$, is adjusted in each figure so that the predictions of (3) reproduce the peaks position in the 0–6 eV energy range. As can be seen in Figs. 6(a)–6(d), the agreement is quite satisfying, thus confirming our interpretation of the origin of the structures in the time-delay calculation. It is noteworthy that the peak energies correspond to quasistationary states, the electron can escape by transmission into vacuum at the cluster border. The peaks in Fig. 6 are rather broad, thus corresponding to a large electron transmission probability at the Ne-vacuum interface. One can also note that only the resonances corresponding to the first zero of the spherical Bessel function are marked by symbols in Fig. 6. Other higher lying resonances associated with the higher zeroes do not appear; apparently, they are associated with smaller peaks. The constant potential $V_0(R)$ determined from Fig. 6 amounts to 1.0 to 1.1eV depending on the adsorption site and cluster size. This does not exactly correspond to the bottom of the Ne bulk conduction band as it has been obtained in the present study (0.95 eV, calculation without mutual polarization). This small difference corresponds to the contribution of the attractive polarization potential of the Ne atoms that, in the complete crystal, lie outside the cluster sphere. This contribution can be simply estimated in a continuous medium approximation and is equal to $(-2\pi\alpha n/R)$, where n is the density of Ne atoms. This difference amounts to −0.16 eV(−0.17 eV) for the nine shells and −0.11eV(−0.12 eV) for the 17 shells at the insertion (substitution) sites, respectively. Taking these energy shifts and the bulk conduction band bottom into account, one then predicts an effective band bottom for the 9(17)-shells cluster, $V_0(R)$, in the (1.06–1.12 eV) range quite consistent with the value (1.0–1.1 eV) obtained from the adjustment in Fig. 6. This again fully confirms our assignment of the peaks in the electronic structure of the cluster and we now have a rather precise picture of the density of states in the cluster: there is a minimum around 7–8 eV surrounded by two maxima around 6 and 9.5 eV and the low energy region which is free-electron like presents a series of oscillations due to the quantization of the electron motion in the finite size cluster.

One can go back now to the interpretation of the structures in the excitation probabilities in Fig. 4 and show that the structures in the excitation probability reflect the cluster density of states. Let us start with the excitation of the $a\ ^1\Delta_g$ state in an insertion site [Figs. 4(a) and 4(c)]. The results for both the nine- and 17-shell clusters exhibit a broad minimum in the region around 8 eV which we can directly connect with the minimum in the density of states visible both in bulk Ne and in the Ne clusters. It appears at an energy slightly higher than in the density of states due to the fact that the electron probes the density of states twice, at the incident and at the outgoing energies. The structures in the low energy part can be attributed to the quantization of the conduction band. Vertical bars in Fig. 4 have been drawn corresponding to the energies expected for the quantized levels [formula (3)]. Since an inelastic process is considered, the quantized levels can appear as initial or final states, so that there are two sets of vertical bars, shifted one with respect to the other by the X-a excitation energy. Since the resonance energy is of $d\pi$ symmetry, it acts as a further filter on the incident wave and we consider now all the possible quantized states associated with a $\ell=2$ wave. The correspondence between the vertical bars and the structures in the excitation probability is satisfying in particular for the 17-shell cluster, although not perfect. Discrepancies can be attributed to defects in the accuracy of formula (3) (in particular, it is not obvious what the effective radius of the cluster is) as well as to possible effects of the coupling of the incident wave to the resonant orbital. The structures at low incident energy do not appear due to a very weak efficiency of the X-a excitation. One can also mention that with the current picture of the process, the electron arrives on the O_2 molecule with an energy decreased by $V_0(R)$ and so the overall excitation probability must be shifted by this quantity, qualitatively accounting for the shifted excitation threshold between the free and the embedded molecules.

The interpretation of the structures in the X-b excitation in the insertion site and in the X-a and b excitation for the substitution site follows along the same line, except for the fact that the structures are shifted to higher energy in the X-b excitation case due to the larger inelasticity of the b excitation. Expected quantization peaks (not shown in the figure for the b state) reproduce the structures in a way similar to the a state. One can notice that the overall shape of the excitation probability is different for the insertion and substitution sites, the latter being smaller at low energy, making the dip in the density of states around 8 eV and the quantized state effects less visible. This is attributed to the different coupling of the propagating states in the cluster with the resonant $d\pi$ wave centered at different places inside the cluster. One can stress that this site effect involves the crystallographic structure of the cluster in contrast with the part of the above interpretation involving the quasifree electron behavior of the conduction band at low energy.

It is worthwhile to mention that similar characteristics are obtained for both embedding sites (insertion and substitution) of the molecule inside the cluster. In both cases, structures appear that are related to properties of the electronic band structure of bulk Ne and of finite size Ne clusters. However coupling with the resonant wave is slightly different for the two embedding sites. A common behavior is then observed for quite different solid environments around the molecule. This indicates that the characteristics that show up in the excitation process are not specific of the particular molecular axis orientation chosen in the present study.

V. CONCLUSIONS

It is well known that the environment of a molecule strongly influences the excitation processes induced by low energy electrons. We considered a model system consisting of an O_2 molecule embedded in a piece of rare gas bulk material, represented by a Ne cluster of variable size. This model system provides the opportunity to study how the electronic properties of the host medium influence the elec-

tron impact excitation processes when the molecule is embedded inside a dielectric medium. Electronic excitation to the two first excited states ($a\ ^1\Delta_g$ and $b\ ^1\Sigma_g^+$) of the oxygen molecule has been calculated. The electron impact excitation probability is deeply modified by the host medium, although it retains the same order of magnitude as for the free molecule. Structures appear in the collision energy dependence of the excitation probabilities that can all be related to properties in the electronic band structure of bulk Ne and of finite size Ne clusters. In particular, the effect of quantization of the quasi-free electron Ne conduction band clearly shows up in the excitation probabilities, both for the incident and for the outgoing electron.

These results in the O_2 in Ne system show that the excitation probabilities reflect directly the host medium density of states. This corresponds to what has been experimentally observed in phonon excitation by electron impact in condensed Ar (Refs. 16,17) and is opposite to the experimental observations for resonant vibrational excitation of O_2 in condensed Ar, where the excitation probability shows an inverse correlation with the density of Ar states.[14,15] This different behavior can be related to the characteristics of the electronic excitation process; the clue is that the present electronic excitation does not present a usual resonant behavior. In the resonant vibrational excitation case, the resonance lifetime is the key parameter, since the longer the lifetime the stronger the vibrational excitation. It was argued[14,15] that the vibrational excitation is increasing with the resonance lifetime which in turn is inversely dependent on the density of states. As a consequence, the excitation probability is exhibiting an inverse correlation with the density of states.[14,15] In contrast, in the present case, the O_2^- resonance lifetime is not really playing a role, the resonant excitation process occurs in the far wing of the resonance profile and it involves a simple coupling-decoupling of the electron angular momenta which is neither favored nor unfavored by a long resonance lifetime (see Refs. 22,42 for a discussion). As a consequence, the excitation probability has a very smooth energy dependence for a free molecule. For the embedded molecule, the probability of the incident electron to travel from vacuum into the Ne cluster and to reach the molecule reflects the cluster density of states thus bringing the correlation that is observed on the present results. The same kind of effect is playing a role in the case of phonon excitation by electron impact in condensed Ar,[16,17] where no resonant behavior bringing a lifetime effect is expected.

Finally, one can stress that the features related to the bulk density of states appear very soon when the size of the cluster increases. Typically, the excitation probabilities for a three-layer cluster (around 40 Ne atoms) already exhibits the gross features of the density of states and, roughly speaking, the changes above three-layer are mainly due to the evolution of the quantification of the conduction band inside the finite size object.

[1] G. J. Schulz, Rev. Mod. Phys. **45**, 423 (1973).
[2] L. Sanche, J. Phys. B **23**, 1597 (1990).
[3] R. E. Palmer and P. J. Rous, Rev. Mod. Phys. **64**, 383 (1992).
[4] R. E. Palmer, Prog. Surf. Sci. **41**, 51 (1992).
[5] J. E. Demuth, D. Schmeisser, and Ph. Avouris, Phys. Rev. Lett. **47**, 1166 (1981).
[6] L. Sanche and M. Michaud, Phys. Rev. Lett. **47**, 1008 (1981).
[7] A. Gerber and A. Herzenberg, Phys. Rev. B **31**, 6219 (1985).
[8] J. W. Gadzuk, J. Chem. Phys. **79**, 3982 (1983).
[9] V. Djamo, D. Teillet-Billy, and J. P. Gauyacq, Phys. Rev. Lett. **71**, 3267 (1993).
[10] V. Djamo, D. Teillet-Billy, and J. P. Gauyacq, Phys. Rev. B **51**, 5418 (1995).
[11] P. J. Rous, Phys. Rev. B **53**, 11 076 (1996).
[12] D. C. Marinica, D. Teillet-Billy, J. P. Gauyacq, M. Michaud, and L. Sanche, Phys. Rev. B **64**, 085408 (2001).
[13] J. P. Gauyacq, A. G. Borisov, and G. Raseev, Surf. Sci. **490**, 99 (2001).
[14] M. Michaud, M. Lepage, and L. Sanche, Phys. Rev. Lett. **81**, 2807 (1998).
[15] M. Michaud, M. Lepage, and L. Sanche, Phys. Rev. B **59**, 15 480 (1999).
[16] M. Michaud, L. Sanche, T. Goulet, and J.-P. Jay-Gerin, Phys. Rev. Lett. **66**, 1930 (1991).
[17] M. Michaud, P. Cloutier, and L. Sanche, Phys. Rev. B **44**, 10 485 (1991).
[18] T. Goulet, J.-M. Jung, M. Michaud, J.-P. Jay-Gerin, and L. Sanche, Phys. Rev. B **50**, 5101 (1994).
[19] F. Linder and Z. Schmidt, Z. Naturforsch. A **26A**, 1617 (1971).
[20] S. Trajmar, D. C. Cartwright, and W. Williams, Phys. Rev. A **4**, 1482 (1971).
[21] T. W. Shyn and C. J. Sweeney, Phys. Rev. A **47**, 1006 (1993).
[22] D. Teillet-Billy, L. Malegat, and J. P. Gauyacq, J. Phys. B **20**, 3201 (1987).
[23] C. J. Noble and P. G. Burke, Phys. Rev. Lett. **68**, 2011 (1992).
[24] C. J. Noble and P. G. Burke, J. Phys. B **19**, L35 (1986).
[25] B. Bahrim, D. Teillet-Billy, and J. P. Gauyacq, J. Chem. Phys. **104**, 10014 (1996).
[26] P. G. Burke, K. Higgins, and J. E. Inglesfield, Philos. Trans. R. Soc. London, Ser. A **357**, 1143 (1999).
[27] J. Farges, M. F. de Feraudy, B. Raoult, and G. Torchet, J. Chem. Phys. **78**, 5067 (1983).
[28] D. Teillet-Billy and J. P. Gauyacq, Surf. Sci. **239**, 343 (1990).
[29] G. Peach, J. Phys. B **11**, 2107 (1978).
[30] J. F. Williams, J. Phys. B **12**, 265 (1979).
[31] T. F. O'Malley and R. W. Crompton, J. Phys. B **13**, 3451 (1980).
[32] H. P. Saha, Phys. Rev. Lett. **65**, 2003 (1990).
[33] D. C. Marinica, C. Ramseyer, A. G. Borisov, D. Teillet-Billy, J. P. Gauyacq, W. Berthold, P. Feulner, and U. Höfer, Phys. Rev. Lett. **89**, 046802 (2002).
[34] D. C. Marinica, C. Ramseyer, A. G. Borisov, D. Teillet-Billy, and J. P. Gauyacq, Surf. Sci. **540**, 457 (2003).
[35] N. C. Bacalis, D. A. Papaconstantopoulos, and W. E. Pickett, Phys. Rev. B **38**, 6218 (1988).
[36] B. Kassühlke, P. Averkamp, S. Frigo, P. Feulner, and W. Berthold, Phys. Rev. B **55**, 10 854 (1997).
[37] N. Schwentner, E. E. Koch, and J. Jortner, *Electronic Excitation in Condensed Rare Gases*, Springer Tracts in Modern Physics

Vol. 107 (Springer-Verlag, Berlin. 1985).
[38] N. Schwentner, F.-J. Himpsel, V. Saile, M. Skibowski, W. Steinmann, and E. E. Koch, Phys. Rev. Lett. **34**, 528 (1975).
[39] J. P. Gauyacq, *Dynamics of Negative Ions* (World Scientific, Singapore, 1987).
[40] M.-C. Desjonquères and D. Spanjaard, *Concept in Surface Physics* (Springer-Verlag, Berlin, 1993).
[41] F. T. Smith, Phys. Rev. **118**, 349 (1960).
[42] D. Teillet-Billy and J. P. Gauyacq, J. Phys. B **22**, L335 (1989).
[43] D. Teillet-Billy, L. Malegat, J. P. Gauyacq, R. Abouaf, and C. Benoit, J. Phys. B **22**, 1095 (1989).